Astrochemistry VII – Through the Cosmos
from Galaxies to Planets
Proceedings IAU Symposium No. 332, 2017
M. Cunningham, T. Millar & Y. Aikawa, eds.

doi:10.1017/S1743921317007591

Chemical Change in the Disk Forming Region of IRAS 16293–2422 Studied with ALMA

Yoko Oya

Department of Physics, The University of Tokyo,
Bunkyo-ku, Tokyo, 113-0033, Japan
email: oya@taurus.phys.s.u-tokyo.ac.jp

Abstract. We have analyzed rotational spectral line emission of OCS, CH_3OH, $HCOOCH_3$, and H_2CS observed toward the low-mass Class 0 protostar IRAS 16293–2422 (Source A and B) at a sub-arcsecond resolution with ALMA. Significant chemical differentiation is found at a 50 au scale. OCS is found to trace the infalling-rotating envelope, while COM distributions are concentrated around the inner part of the envelope. The kinematic structure in Source A is explained with a ballistic model, and the protostellar mass and the radius of the centrifugal barrier are evaluated to be $\sim$0.75 $M_\odot$ and $\sim$50 au, respectively. This study has revealed that the centrifugal barrier plays a central role not only in the disk formation but also in the associated chemical evolution.

Keywords. ALMA, IRAS 16293–2422, Molecules, Disk formation

1. Introduction

1.1. *Chemical Diversity of Protostellar Envelopes*

In star-formation studies, disk formation is an important subject. However, it is still controversial *when and how disks are formed from envelopes*, and also, *how molecules in envelopes are delivered into disks*. To answer these questions, we are conducting a chemical analysis of disk forming regions. It is well known that the chemical composition of the protostellar envelopes shows a significant diversity (Sakai & Yamamoto 2013). One distinct case is warm carbon-chain chemistry, which is rich in unsaturated carbon-chain molecules. Another distinct case is hot corino chemistry, which is rich in saturated organic molecules. How such a chemical diversity evolves into the disk is an interesting issue for astrochemistry. At the same time, chemical diagnostics can give us important information on physical processes in disk formation. Here, we report about such a chemical analysis toward a very famous source, IRAS 16293–2422.

1.2. *IRAS 16293–2422*

This source is a well-studied low-mass Class 0 protostar in Ophiuchus (d = 120 pc; Knude & Hog 1998). It is rich in saturated complex organic molecules (COMs), such as $HCOOCH_3$ and $(CH_3)_2O$, in the vicinity of the protostars (e.g., Schöier *et al.* 2002; Cazaux *et al.* 2003; Bottinelli *et al.* 2004a; Kuan *et al.* 2004; Pineda *et al.* 2012; Jørgensen *et al.* 2012, 2016). With this characteristic chemical composition, this source is very famous as the prototypical hot corino source (Ceccarelli 2004; Bottinelli *et al.* 2004a). Toward Source A, a rotating motion is reported (e.g. Pineda *et al.* 2012; Favre *et al.* 2014). We analyzed an archival data toward this source in ALMA Cycle 1 (ADS/JAO.ALMA #2012.1.00712.S) to investigate this rotating motion in detail. We analyzed the spectral lines of OCS (J=19–18), CH_3OH ($11_{0,11}$–$10_{1,10}$; A^+), $HCOOCH_3$ ($19_{9,10}$–$19_{8,11}$; E),

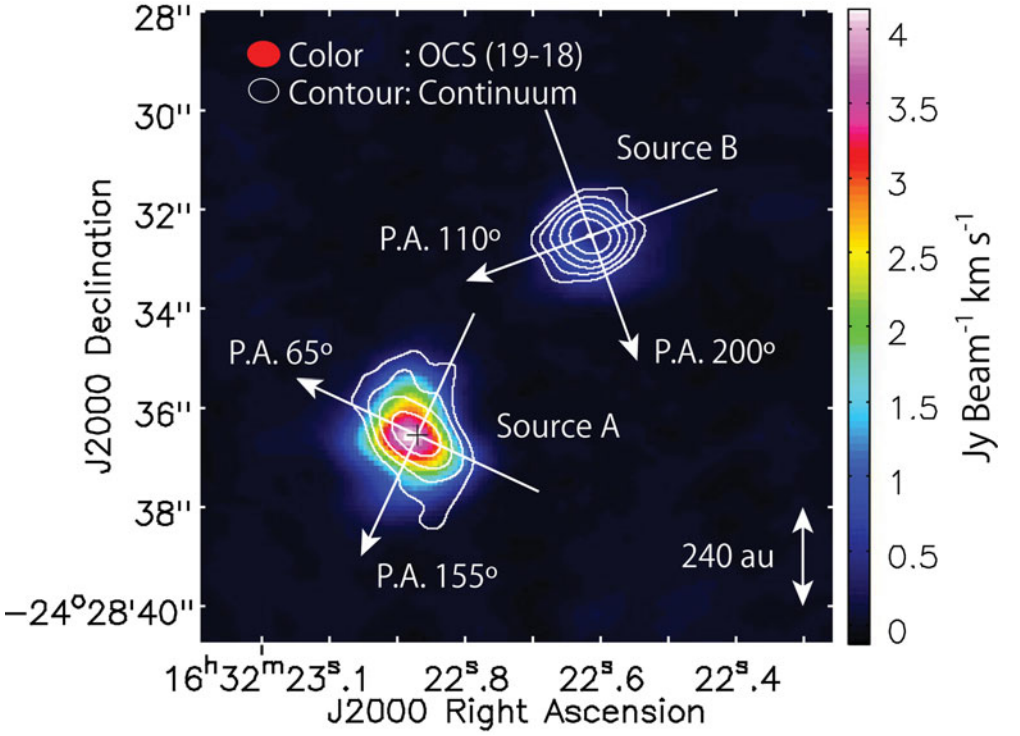

Figure 1. Integrated intensity map of the OCS (color; J=19–18) and the 1.2 mm continuum map (contours). The contour levels for the continuum are 10, 20, 40, 80, 160, and 320σ, where the rms noise level is 2 mJy beam^{-1}. White arrows on Source A represent the direction along its disk/envelope system (P.A. 65°) and one perpendicular to it (P.A. 155°). A black cross represents the protostellar position of Source A. White arrows on Source B represent the direction along its disk/envelope system (P.A. 110°) and one perpendicular to it (P.A. 200°).

and H_2CS ($7_{0,7}$–$6_{0,6}$; $7_{2,5}$–$6_{2,4}$; $7_{4,4}$–$6_{4,3}$, $7_{4,3}$–$6_{4,2}$) in Band 6 ($\sim$ 250 GHz). A typical resolution is 0.″5 ($\sim$ 60 au).

2. Envelope and Disk Structures in Source A

2.1. *Envelope Traced by OCS*

Figure 1 shows the integrated intensity map of the OCS (J=19–18) line. The white arrows represent the direction along which the mid-plane of the disk/envelope system is extended (P.A. 65°) and the line perpendicular to it (P.A. 155°). We prepared the position-velocity (PV) diagrams of OCS (Figures 2a, b) to analyze the kinematic structure of the gas in Source A. In the diagram prepared along the disk/envelope system (Figure 2a), there is a velocity gradient indicating the rotating motion. In addition, a velocity gradient perpendicular to the envelope can also be seen (Figure 2b), which indicates the infall motion. Thus, the kinematic structure of OCS cannot be explained by the Keplerian motion, which does not have the infall motion. In order to interpret these kinematic structures, we consider the infall and rotation motion in the envelope.

Figure 3 shows a schematic illustration of a ballistic model of an infalling-rotating envelope (Oya *et al.* 2014). In this model, the gas is falling and rotating under the gravity of the central protostar. Because of energy and angular momentum conservation, the gas cannot fall inward of a certain radius, or the 'perihelion'. Thus, the distribution of the

https://doi.org/10.1017/S1743921317007591 Published online by Cambridge University Press

gas has a hole in this model. This position is called as a 'centrifugal barrier'. This model considers only the central part (a few 100 au) of a whole envelope. It does not involve the Keplerian disk component, which probably exists inside the centrifugal barrier. We calculated the kinematic structure of the envelope with this model.

The results of the infalling-rotating envelope model are shown in Figures 2(a, b). This model seem to reproduce the kinematic structure of OCS along the two directions simultaneously. Comparing the observation with this model, we evaluated the protostellar mass (M) and the radius of the centrifugal barrier ($r_{\rm CB}$) to be from 0.5 to 1.0 $M_\odot$ and from 40 to 60 au, respectively, assuming the inclination angle (i) of 60° (0° for a face-on configuration). This protostellar mass is slightly larger than a previous report by Favre *et al.* (2014) (0.49 $M_\odot$ derived from the $C^{17}O$ observation).

2.2. *Chemical Differentiation*

We also investigated some other molecular lines toward IRAS 16293–2422 Source A: the CH_3OH ($11_{0,11}$–$10_{1,10}$; A^+), $HCOOCH_3$ ($19_{9,10}$–$19_{8,11}$; E), and H_2CS ($7_{0,7}$–$6_{0,6}$) lines (Figures 2c–h). The kinematic structures revealed by these lines are apparently different from that of the OCS line. First, CH_3OH and $HCOOCH_3$ have more compact distributions concentrated around the centrifugal barrier, as seen in the SO line in L1527 (Sakai *et al.* 2014a,b). On the other hand, H_2CS traces the envelope component as OCS does. In addition, H_2CS shows high velocity-shift components concentrated to the protostellar position.

The results of the infalling-rotating envelope model are shown by blue contours in Figure 2. In these models, the physical parameters (e.g., M of 0.75 $M_\odot$, $r_{\rm CB}$ of 50, and i of 60°) are common for all the molecular lines, except for the outer radius of the envelope. Smaller outer radii are appropriate for the CH_3OH (80 au) and $HCOOCH_3$ (55 au) cases. This means that the emitting regions of these lines have ring-like structures around the centrifugal barrier. In addition, the high velocity-shift components of H_2CS can be explained by the Keplerian motion with the protostellar mass derived from the OCS analysis (Figures 2g, h).

The above chemical differentiation can be schematically illustrated like Figure 4(a); OCS traces the envelope, while CH_3OH and $HCOOCH_3$ highlight the centrifugal barrier. These molecules are possibly processed or trapped onto the dust surface while they are being delivered into the disk. On the other hand, H_2CS traces the Keplerian disk component inside the centrifugal barrier in addition to the envelope component. This chemical change is very important in understanding the chemical evolution from the envelope to the disk.

2.3. *Physical/Chemical Changes across the Centrifugal Barrier*

Why is the emitting region different from molecule to molecule? To address this question, we derived the gas kinetic temperature in the envelope component, the centrifugal barrier, and the disk component. The result is shown in Table 1. The gas kinetic temperature increases from the envelope to the centrifugal barrier, and it goes down again in the disk. If the mid-plane temperature is as low as the gas kinetic temperature in the disk ($\sim$ 80 K), COMs would be adsorbed onto dust grains. Therefore, this change in the temperature could be the reason why COMs are bright only at the centrifugal barrier.

We also evaluated the abundance ratio of CH_3OH and $HCOOCH_3$. Assuming the rotation temperature to be around the derived gas kinetic temperatures, the ratios are derived as shown in Table 1. The high abundance ratio of $N(HCOOCH_3)$ / $N(CH_3OH) \sim (0.8-8.7)$ is consistent with a previous report (Bottinelli *et al.* 2007). More interestingly,

https://doi.org/10.1017/S1743921317007591 Published online by Cambridge University Press

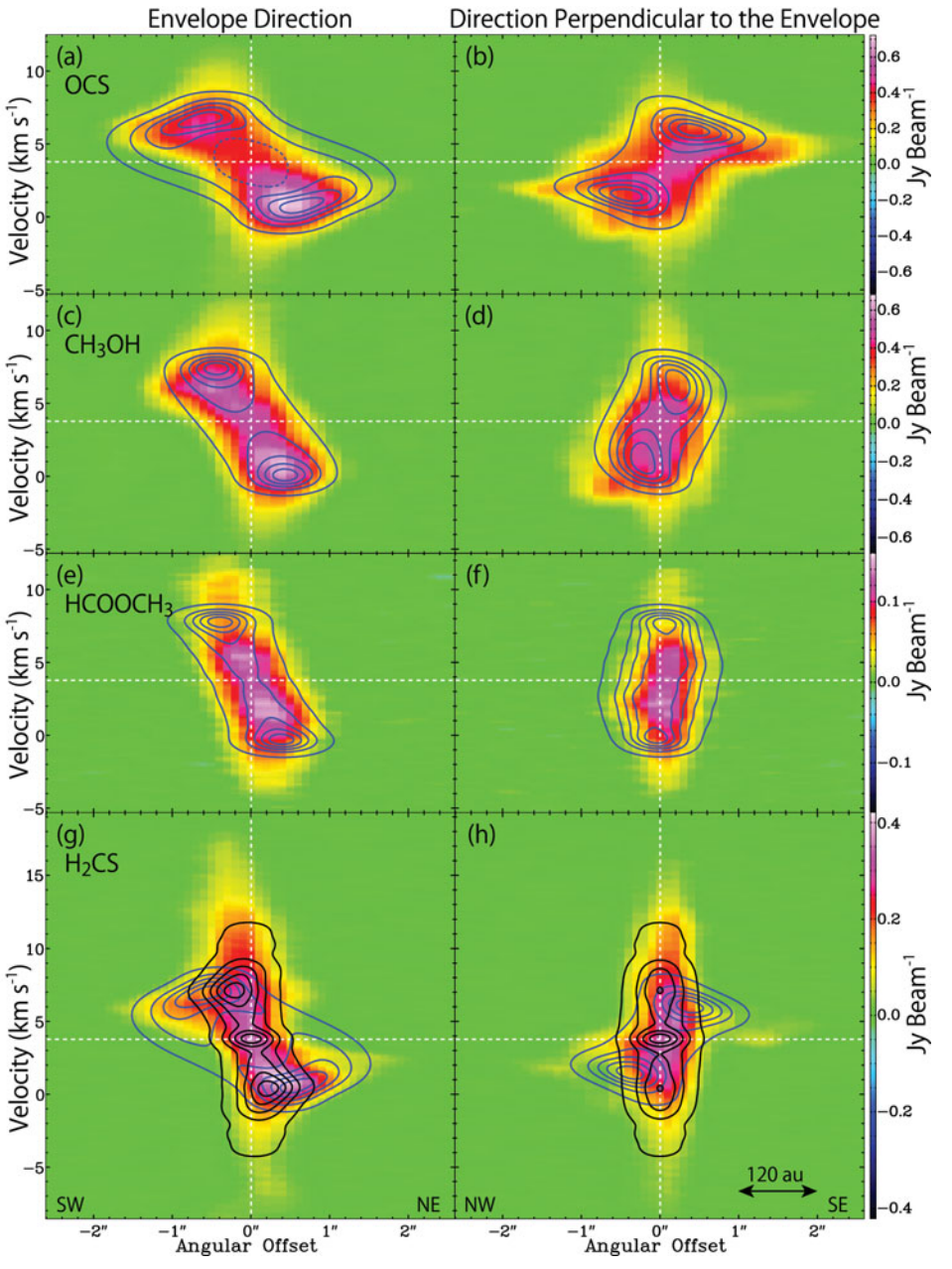

Figure 2. PV diagrams of the OCS (a, b; J=19–18; 231.061 GHz), CH_3OH (c, d; $11_{0,11}$–$10_{1,10}$; A^+; 250.507 GHz), $HCOOCH_3$ (e, f; $19_{9,10}$–$19_{8,11}$; E; 232.597 GHz), and H_2CS (g, h; $7_{0,7}$–$6_{0,6}$; 240.267 GHz) lines. The position axes are along the disk/envelope system (a, c, e, g; P.A. 65°) and the direction perpendicular to it (b, d, f, h; P.A. 155°). The vertical white dotted lines represent the protostellar position, and the horizontal ones represent the systemic velocity of Source A ($\sim$ 3.8 km s^{-1}; e.g., Favre *et al.* 2014). Blue contours represent the results of the infalling-rotating envelope model with the following physical parameters: M of 0.75 $M_\odot$, r_{CB} of 50, and i of 60°. The scale height of the envelope is assumed to increase as the distance from the protostar with the extending angle of 45°. The outer radius of the envelope model is set to be 180, 80, 55, and 150 au for the OCS, CH_3OH, $HCOOCH_3$, and H_2CS lines, respectively, so as to demonstrate the molecular distributions. Black contours in panels (g, h) represent the Keplerian model with the protostellar mass of 0.75 $M_\odot$ and the inclination angel of 60°.

https://doi.org/10.1017/S1743921317007591 Published online by Cambridge University Press

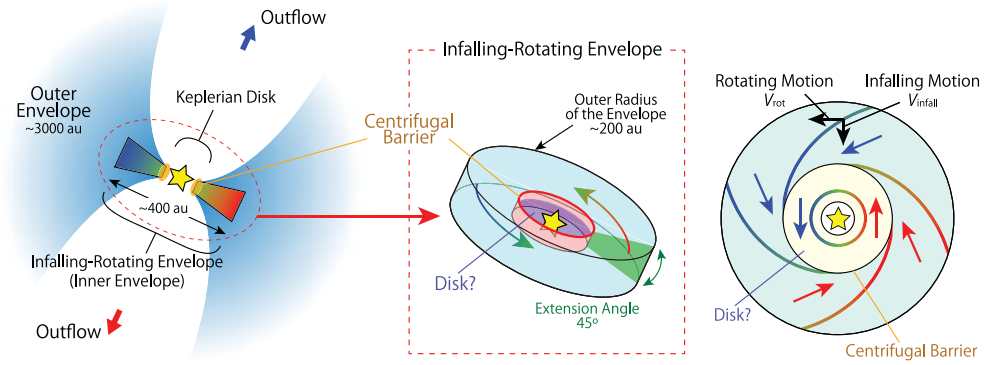

Figure 3. Schematic illustration of the gas components around Source A. The outer envelope part represented by light blue regions in the left figure is resolved out in these observations. The gas components are roughly divided into the infalling-rotating envelope and the disk component by the centrifugal barrier.

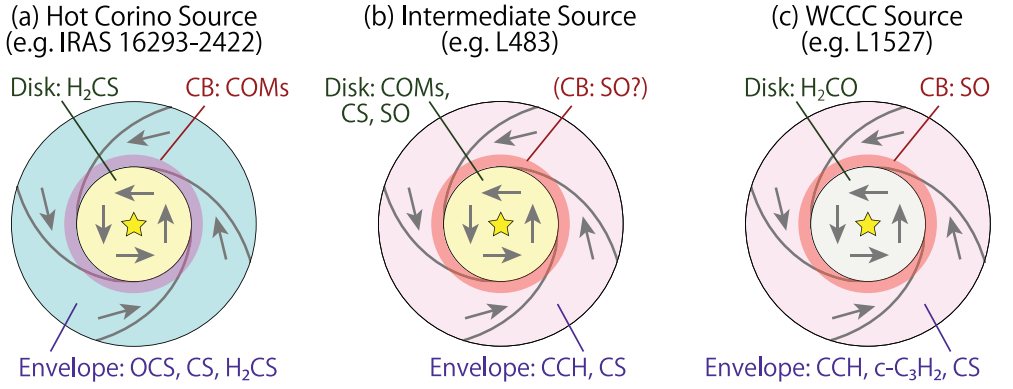

Figure 4. Schematic illustration of the chemical differentiation across the centrifugal barrier.

Table 1. Physical Parameters

	Envelope	Centrifugal Barrier	Disk
Gas Kinetic Temperature[a]	$70-110$	$110-140$	$70-90$
Abundance Ratio[b]	0.8 ± 0.5	4.2 ± 0.3	8.7 ± 1.3

[a] In K. The gas kinetic temperatures are derived from the intensity ratio of the H_2CS ($7_{0,7}$–$6_{0,6}$; $7_{2,5}$–$6_{2,4}$) lines by using RADEX code (van der Tak *et al.* 2007). The assumed ranges for the H_2 density and the column density of H_2CS are from 10^7 to 10^9 cm^{-3} and from 10^{13} to 10^{15} cm^{-2}, respectively. The error is estimated only from the statistical error and does not contain the calibration error, because it will be almost canceled in the intensity ratios.

[b] The abundance ratio of $HCOOCH_3$ to CH_3OH derived under the LTE approximation. The quoted errors represent 3σ, which are estimated from the rms noise level.

the abundance ratio systematically increases from the envelope to the disk. Its origin is puzzling, and is subject to chemical modeling of the disk forming region.

2.4. *Summary for Source A*

In this analysis, the basic structure of the envelope is found to be reproduced by a simple ballistic model. Moreover, we find that significant physical and chemical changes are

https://doi.org/10.1017/S1743921317007591 Published online by Cambridge University Press

occurring around the centrifugal barrier. First, the gas kinetic temperature is highest at the centrifugal barrier. This can be caused by thermal heating by the protostar and a weak accretion shock by the infalling gas. The chemical composition also changes from the envelope to the disk. Therefore, the next target is the more detailed structure in the 'transition zone' from the envelope to the disk, which will be investigated at a higher angular resolution observation in the future.

3. IRAS 16293–2422 Source B Case

We also analyzed the molecular distributions in IRAS 16293–2422 Source B. Figure 5 shows the PV diagrams centered at the protostar in Source B. All of the molecular lines show an inverse P-Cygni profile, which implies the infall motion. The distributions of the OCS and H_2CS lines are extended in a 400 au scale. On the other hand, that of the CH_3OH line is more concentrated in a 200 au scale. This chemical differentiation is similar to the Source A case. Detailed analyses of their kinematic structure by the infalling-rotating envelope model are in progress.

4. Discussion

4.1. *Infalling-Rotating Envelope in Low-Mass Protostellar Sources*

In addition to IRAS 16293–2422 Source A and Source B studied above, we have demonstrated that the infalling-rotating envelope model explains the kinematic structure of other sources, L1527, IRAS 15398–3359, TMC–1A, and L483 (Sakai *et al.* 2014a,b, 2016; Oya *et al.* 2014, 2015, 2017). We derived the physical parameters in the infalling-rotating envelope model for these sources. With the aid of this model, we also found the chemical change at the centrifugal barrier in the above sources, as shown in Figure 4.

4.2. *Transition Zone from Envelopes to Disks*

Generally, the disk radius is thought to be close to the centrifugal radius, where the Keplerian velocity equals to the rotation velocity. This radius is the twice the radius of the centrifugal barrier. However, the simple ballistic model well reproduces the kinematic structure in IRAS 16293–2422 Source A and the other sources mentioned above. This means that the gas keeps falling toward the centrifugal barrier to some extent. However, our model is too simplified, and we need to consider various effects, such as the gas pressure, the magnetic field effect, the self-gravity, and the time variation of the angular momentum of the gas. They will affect where the infall motion of the gas practically vanishes. Considering these complex situations, it is still unknown *what is occurring between the centrifugal radius and the centrifugal barrier*. This is a really interesting problem left for the future studies.

4.3. *Chemical Diversity in Disk Forming Regions*

In the binary system, IRAS 16293–2422, we found a drastic change in the chemical composition of the gas around the centrifugal barrier. Such a chemical differentiation is also seen in other low-mass protostellar sources with different chemical characteristics (Figure 4). These chemical changes at the centrifugal barrier will affect the initial condition for chemical evolution in the disk formation, and eventually, the material environment of the possible planets formed in the future. The chemical differentiation in the disk forming region provides us with an essential clue to understanding the total chemical processes during the disk formation.

https://doi.org/10.1017/S1743921317007591 Published online by Cambridge University Press

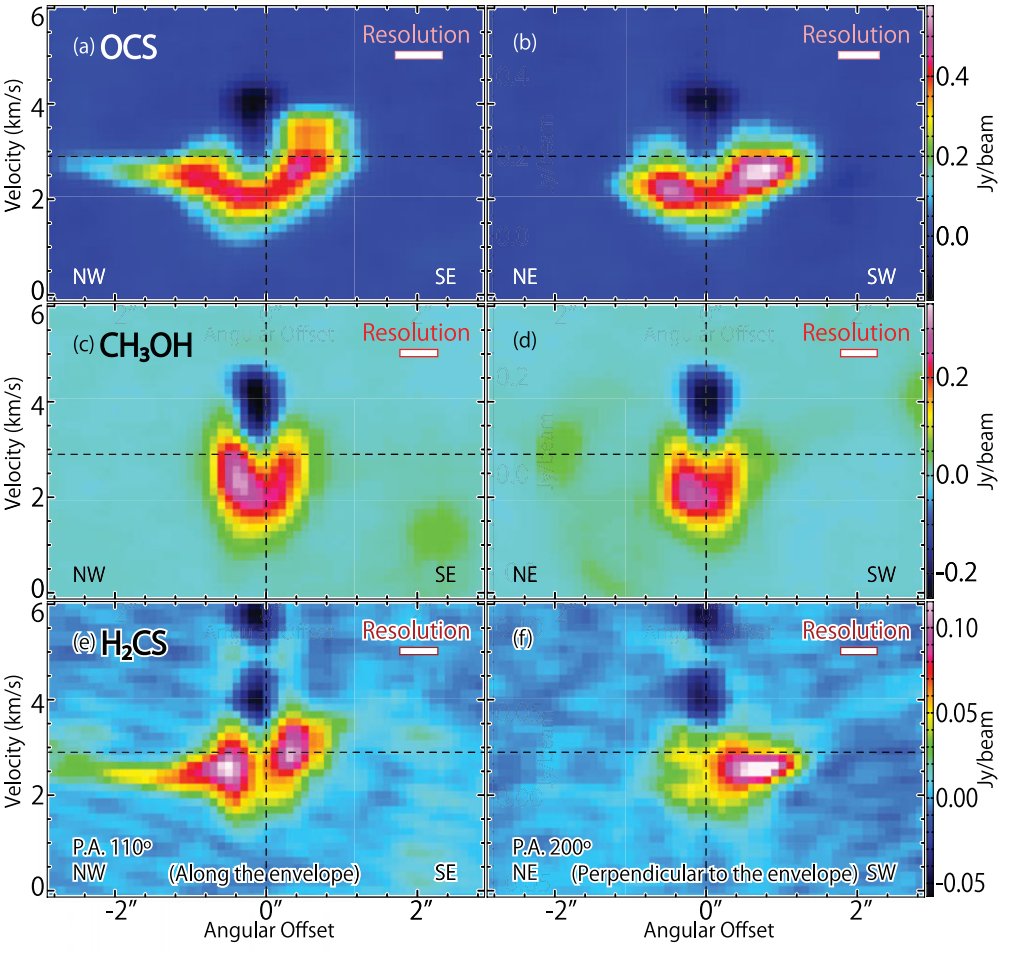

Figure 5. PV diagrams of the OCS (a, b; J=19–18), CH_3OH (c, d; $5_{1,5}$–$4_{1,4}$; A^+), and H_2CS (e, f; $7_{0,7}$–$6_{0,6}$) lines. The position axes are along the disk/envelope system (P.A. 110°) and the direction perpendicular to it (P.A. 200°) in Source B. The vertical black dotted lines represent the protostellar position, while the horizontal ones represent the systemic velocity of Source B ($\sim$ 2.9 km s^{-1}).

Acknowledgement

The author thanks Nami Sakai, Ana López-Sepulcre, Yoshimasa Watanabe, Cecilia Ceccarelli, Bertrand Lefloch, Cécile Favre, and Satoshi Yamamoto for invaluable discussions.

References

Bottinelli, S., Ceccarelli, C., Neri, R., *et al.* 2004a, ApJ, 617, L69
Bottinelli, S., Ceccarelli, C., Williams, J. P., & Lefloch, B. 2007, A&A, 463, 601
Cazaux, S., Tielens, A. G. G. M., Ceccarelli, C., *et al.* 2003, ApJ, 593, L51
Ceccarelli, C. 2004, Star Formation in the Interstellar Medium: In Honor of David Hollenbach, 323, 195
Favre, C., Jørgensen, J. K., Field, D., *et al.* 2014, ApJ, 790, 55
Jørgensen, J. K., Favre, C., Bisschop, S. E., *et al.* 2012, ApJ, 757, L4

https://doi.org/10.1017/S1743921317007591 Published online by Cambridge University Press

Jørgensen, J. K., van der Wiel, M. H. D., Coutens, A., *et al.* 2016, A&A, 595, A117
Knude, J. & Hog, E. 1998, A&A, 338, 897
Kuan, Y.-J., Huang, H.-C., Charnley, S. B., *et al.* 2004, ApJ, 616, L27
Oya, Y., Sakai, N., Sakai, T., *et al.* 2014, ApJ, 795, 152
Oya, Y., Sakai, N., Lefloch, B., *et al.* 2015, ApJ, 812, 59
Oya, Y., Sakai, N., López-Sepulcre, A., *et al.* 2016, ApJ, 824, 88
Oya, Y., Sakai, N., López-Sepulcre, A., *et al.* 2017, ApJ, 837, 174
Pineda, J. E., Maury, A. J., Fuller, G. A., *et al.* 2012, A&A, 544, L7
Sakai, N., Sakai, T., Hirota, T., *et al.* 2014a, Nature, 507, 78
Sakai, N., Oya, Y., Sakai, T., *et al.* 2014b, ApJ, 791, L38
Sakai, N., Oya, Y., López-Sepulcre, A., *et al.* 2016, ApJ, 820, L34
Sakai, N. & Yamamoto, S. 2013, Chemical Reviews, 113, 8981
Schöier, F. L., Jørgensen, J. K., van Dishoeck, E. F., & Blake, G. A. 2002, A&A, 390, 1001
van der Tak, F. F. S., Black, J. H., Schöier, F. L., Jansen, D. J., & van Dishoeck, E. F. 2007, A&A, 468, 627

https://doi.org/10.1017/S1743921317007591 Published online by Cambridge University Press